Cell Cycle 14:19, 3163–3172; October 1, 2015; © 2015 Taylor & Francis Group, LLC

Chibby functions to preserve normal ciliary morphology through the regulation of intraflagellar transport in airway ciliated cells

Saul S Siller[1,2,3,†], Michael C Burke[1,4,†], Feng-Qian Li[2,3], and Ken-Ichi Takemaru[1,2,3,4,*]

[1]Medical Scientist Training Program; Stony Brook University; Stony Brook, NY USA; [2]Graduate Program in Molecular and Cellular Pharmacology; Stony Brook University; Stony Brook, NY USA; [3]Department of Pharmacological Sciences; Stony Brook University; Stony Brook, NY USA; [4]Graduate Program in Genetics; Stony Brook University; Stony Brook, NY USA

[†]These authors contributed equally to this work.

Keywords: axoneme, cilia, ciliary maintenance, Chibby, intraflagellar transport, multiciliated cells, trachea

Airway cilia provide the coordinated motive force for mucociliary transport, which prevents the accumulation of mucus, debris, pollutants, and bacteria in our respiratory tracts. As airway cilia are constantly exposed to the environment and, hence, are an integral component of the pathogenesis of several congenital and chronic pulmonary disorders, it is necessary to understand the molecular mechanisms that control ciliated cell differentiation and ciliogenesis. We have previously reported that loss of the basal body protein Chibby (Cby) results in chronic upper airway infection in mice due to a significant reduction in the number of airway cilia. In the present work, we demonstrate that Cby is required for normal ciliary structure and proper distribution of proteins involved in the bidirectional intraflagellar transport (IFT) system, which consists of 2 distinct sub-complexes, IFT-A and IFT-B, and is essential for ciliary biogenesis and maintenance. In fully differentiated ciliated cells, abnormal paddle-like cilia with dilated ciliary tips are observed in Cby−/− airways and primary cultures of mouse tracheal epithelial cells (MTECs). In addition, IFT88, an IFT-B sub-complex protein, robustly accumulates within the dilated tips of both multicilia in Cby−/− MTECs and primary cilia in Cby−/− mouse embryonic fibroblasts (MEFs). Furthermore, we show that only IFT-B components, including IFT20 and IFT57, but not IFT-A and Bardet-Biedl syndrome (BBS) proteins, amass with IFT88 in these distended tips in Cby−/− ciliated cells. Taken together, our findings suggest that Cby plays a role in the proper distribution of IFT particles to preserve normal ciliary morphology in airway ciliated cells.

Introduction

Cilia are ancient microtubule-based organelles that are integral to various important cellular functions.[1] Two main categories of cilia exist: primary cilia or multicilia, which are defined by a 9 + 0 or 9 + 2 microtubule arrangement, respectively.[2] Primary cilia are generally immotile and function in signaling or specialized sensory transduction processes, i.e. photoreception, mechanosensation.[3] An exception is the primary cilia of the embryonic node, which beats in a rotational fashion to generate leftward fluid flow and establish left-right body patterning during vertebrate embryonic development. Dysfunction of primary cilia leads to a wide spectrum of diseases, collectively known as the ciliopathies that include Bardet-Biedl syndrome (BBS), Joubert syndrome, and polycystic kidney disease.[4] On the other hand, multiciliated cells have hundreds of motile cilia per cell and perform specialized functions, such as mucociliary clearance in the respiratory tract, transport of the ovum through the fallopian tube, and cerebrospinal fluid movement in the ventricular system of the brain.[5] As such, the hallmark symptoms of the classical congenital multicilia disorder primary ciliary dyskinesia (PCD) are chronic sinusitis and rhinitis, otitis media, hydrocephalus, infertility, and *situs inversus*.[6] Additionally, defective multicilia have been implicated as part of the pathogenesis of multiple chronic pulmonary conditions, including cystic fibrosis, asthma, and chronic obstructive pulmonary disease.[7] Consequently, understanding how cilia are assembled and maintained in the airway epithelium is critical for prevention and treatment of such diseases.

The nucleation of both primary and multicilia from a basal body, a modified mother centriole, follows a largely analogous process while the mode of centriole replication differs.[8-10] In cycling cells, a pair of centrioles forms the centrosome, which duplicates once per cell cycle directly from the pre-existing centrioles (the canonical centriolar pathway). In multiciliated cells, centrioles are generated through both centriolar and acentriolar pathways. The acentriolar pathway produces the vast majority of centrioles in multiciliated cells on fibrogranular structures termed deuterosomes, which act as sites of

*Correspondence to: Ken-Ichi Takemaru; Email: ken-ichi.takemaru@stonybrook.edu
Submitted: 04/14/2015; Revised: 07/21/2015; Accepted: 08/02/2015
http://dx.doi.org/10.1080/15384101.2015.1080396

de novo centriole replication.[11-13] After centriole duplication occurs, the nascent centriole acquires both sub-distal and distal appendage structures to mature into a basal body competent to extend a ciliary axoneme.[14] Several reports demonstrate the importance of the distal appendage structure in the recruitment of small vesicles,[15-18] which subsequently fuse to form a large membranous cap called the ciliary vesicle.[12,19,20] Ciliary vesicles then fuse with the apical plasma membrane, which facilitates basal body docking. After attachment at the apical cell membrane, the distal appendages transform into the transition fibers, which are thought to serve as docking sites for intraflagellar transport (IFT) particles.[14,21] At this point, the basal body is poised to extend and maintain a ciliary axoneme.

IFT is the bidirectional transport system that moves cargo proteins along the cilium.[22,23] First discovered in *Chlamydomonas reinhardtii*, IFT is essential for ciliary growth, structure, and maintenance through the delivery of tubulins and other axonemal components to their sites of incorporation within the ciliary compartment. With more than 20 core protein subunits, 2 major IFT sub-complexes have been identified: the (1) IFT-B and (2) IFT-A sub-complexes.[24,25] IFT-B is thought to mediate anterograde transport in association with kinesin motors while IFT-A is implicated in retrograde transport via dynein motors. Besides the requisite association of IFT proteins with kinesin and dynein motors, IFT particles associate and co-migrate with the BBSome along cilia.[26-29] Originally identified as mutated in BBS, the BBSome is an octameric complex that consists of 8 conserved BBS proteins and that has been proposed to regulate the assembly, rearrangement, and turnaround of IFT particles at both the ciliary base and tip.[26,30-32] However, beyond the BBSome components, a limited number of regulators of IFT particle assembly, rearrangement, and turnaround are known.

Chibby (Cby) is a small, evolutionarily conserved 15-kDa coiled-coil protein critical for ciliogenesis.[33,34] We reported that Cby−/− mice develop chronic airway infection due to impaired mucociliary clearance caused by a significant decrease in the number of multicilia in the airway epithelium.[34,35] In addition to phenotypes related to multicilia, Cby−/− mice show cystic kidneys as a result of defective primary cilia,[36] suggesting a conserved function for Cby in both primary and multicilia. Consistent with these results, we demonstrated that Cby predominantly localizes to the basal body at the transition fiber/proximal transition zone region of cilia through several modalities, including immuno-electron microscopy and super-resolution microscopy.[15,37] These findings have also been confirmed in both *Drosophila melanogaster* and *Xenopus laevis*.[38,39]

We previously reported that the loss of cilia in mature Cby−/− airway ciliated cells coincides with the presence of many undocked basal bodies in the apical cytoplasm.[34,35] Recently, we found that this basal body docking defect results from a failure to efficiently recruit and fuse small vesicles to form ciliary vesicles at the distal appendage in the absence of Cby.[15] On a molecular level, Cby is recruited to the basal body by the distal appendage protein CEP164 and stabilizes the interaction between CEP164 and Rabin8,[15] a guanine nucleotide exchange factor (GEF) for the small GTPase Rab8.[40] Rabin8 is then able to promote the local recruitment and activation of Rab8, which facilitates ciliary vesicle assembly at the basal body during early differentiation stages.[40-42] Interestingly, Cby continues to reside at the ciliary base, even after ciliogenesis is complete, in fully differentiated ciliated cells. However, it is unknown if Cby functions during later stages of differentiation or in maintenance of airway ciliated cells.

Here, we report that Cby functions in the regulation of IFT particle localization along cilia to maintain proper ciliary structure and morphology. Cby−/− airway ciliated cells develop a fraction of cilia with a paddle-like morphology and a dilated ciliary tip both *in vivo* and *in vitro*. We show that the IFT-B protein IFT88 accumulates within these tip distortions in both primary and multicilia. Additionally, we demonstrate that the other IFT-B proteins IFT20 and IFT57 accumulate with IFT88 at the ciliary tip while the IFT-A protein IFT140 and the BBSome components BBS4 and BBS5 do not. These findings indicate that Cby plays an integral role in the modulation of IFT protein localization and ciliary structure. Taken together with the finding that Cby localizes predominantly at the ciliary base, we propose that Cby is involved in proper IFT particle assembly at the ciliary base. Hence, loss of Cby would affect IFT particle composition, which leads to defects in IFT particle rearrangement at the ciliary tip and the abnormal ciliary morphology observed in Cby−/− airway ciliated cells.

Results

Loss of Cby leads to dilated distal tips of cilia in airway ciliated cells

To investigate the effect of loss of Cby on mature airway cilia, we performed scanning electron microscopy (SEM) of Cby+/+ and Cby−/− adult mouse bronchial epithelium (**Fig. 1**, *In vivo*). Consistent with our previous findings,[15,34,35] the number of cilia

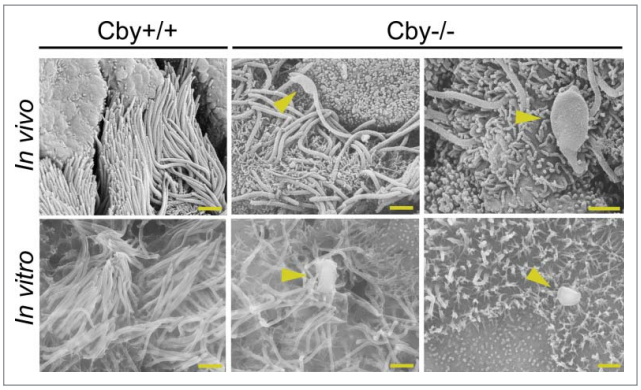

Figure 1. Ciliated cells of Cby−/− airways display a bulge morphology at the ciliary tip. Shown are scanning electron micrographs of adult Cby+/+ (left column) and Cby−/− (middle and right columns) mouse bronchial airways (*In vivo*; top row) and ALId21 MTECs (*In vitro*; bottom row). Both Cby−/− bronchial airways and MTECs demonstrated a paddle-like ciliary morphology with dilated distal tips (arrowheads). In addition to cilia, the apical surface of ciliated cells contains numerous microvilli. Scale bars: 1 μm.

in Cby−/− airways was reduced when compared to Cby+/+ airways. Surprisingly, in a fraction of cilia present on Cby−/− bronchi, we found abnormalities in ciliary structure at the distal end. These ciliary malformations displayed a characteristic paddle-like morphology with a large, distended distal tip structure (**Fig. 1**, arrowheads). The dramatic ballooning of the ciliary tip was an infrequent event in the Cby−/− bronchus; however, such ciliary structural defects were not observed in Cby+/+ bronchus. Thus, despite their low frequency, these dilations of the ciliary tip were specific for the loss of Cby.

To determine if similar paddle-like cilia with dilated distal tips could be found *in vitro*, we exploited the well-established mouse tracheal epithelial cell (MTEC) primary culture system.[10,43-45] To generate primary cultures of MTECs, isolated tracheal cells were seeded at low density onto a semipermeable, collagen-coated membrane and subsequently allowed to proliferate for ≤7 days. Once confluent, an air-liquid interface (ALI) was created to induce multiciliated cell differentiation. As we reported previously,[15] at 9–14 days post-ALI induction (ALId9–14), a majority of Cby+/+ cells were fully differentiated while Cby−/− MTECs showed a reduction in the number of fully differentiated cells and of cilia per ciliated cell (data not shown). A similar trend for both Cby+/+ and Cby−/− MTECs was maintained at ALId21 (data not shown). We then performed SEM on Cby+/+ and Cby−/− MTECs at ALId21 to assess whether paddle-like cilia could be observed. As shown in **Figure 1** (*In vitro*), Cby−/− MTECs displayed an atypical ciliary morphology with dilated distal tips similar to the defects seen in Cby−/− bronchi *in vivo* (**Fig. 1**, arrowheads). Also, similar to the bronchus, despite the low frequency of the structural abnormalities, the formation of these distended ciliary tips and paddle-like cilia were not seen in Cby+/+ MTECs. These findings suggest that Cby is critical for proper ciliary architecture in mature airway ciliated cells.

The IFT-B subunit IFT88 aggregates in Cby−/− airway ciliated cells

The IFT system plays an essential role in the biogenesis and maintenance of cilia via trafficking of cargo proteins along axonemal microtubules.[22,28,46] Prior studies have demonstrated that mutations in the genes that encode for IFT-A components lead to a ciliary bulge morphology, which often contains vesicular accumulation in the dilated distal tips.[28,47-54] Specific examples include IFT122 mutants in *Tetrahymena thermophila* and mice and IFT144 mutants in *C. reinhardtii* and mice.[48,49,52,53] Beyond IFT, mutants for the motor constituents dynein heavy and light chains and multiple BBSome components in *C. reinhardtii* and mice have also exhibited bulge phenotypes.[50,55-57] We therefore hypothesized that IFT-associated proteins are misregulated in fully differentiated Cby−/− ciliated cells with paddle-like cilia. To examine this possibility, we performed immunofluorescence (IF) staining of IFT88, an IFT-B subunit,[22,24,28] in ALId21 Cby+/+ and Cby−/− MTECs (**Fig. 2A**). In Cby+/+ MTECs, intense IFT88 signals were detectable at the basal body with weak punctate signals also present along the ciliary axoneme.[58] In contrast, we detected aberrant accumulations of IFT88 in Cby−/− ciliated cells (**Fig. 2A**, arrowheads). IFT88 aggregations were significantly more frequently observed in Cby−/− ciliated cells (18.2 ± 3 .5% of ciliated cells) compared to Cby+/+ ciliated cells (1.7 ± 0 .3% of ciliated cells) ($p < 0.05$; $n = 4$) (**Fig. 2B**). Interestingly, the numbers of large IFT88 accumulations per ciliated cell were highly variable with a range of 1 to 10 bulges. Next, we assessed IFT88 protein levels in ALId21 Cby+/+ and Cby−/− MTEC lysates by immunoblotting to determine if IFT88 aggregates were caused by alterations in protein expression (**Fig. 2C**). No apparent differences in IFT88 protein levels were detectable between Cby+/+ and Cby−/− MTECs, suggesting that the accumulation of IFT88 in Cby−/− ciliated cells is primarily a localization defect.

We then attempted to rescue the IFT88 accumulation phenotype with lentivirus-mediated expression of Flag-tagged full-length human Cby (hCby) (**Fig. 2D**). In ALId21 Cby−/− MTECs, many infected ciliated cells demonstrated normal IFT88 localization patterns (when compared to Cby+/+ ciliated cells in **Fig. 2A**). However, neighboring uninfected Cby−/− ciliated cells displayed IFT88 accumulations (**Fig. 2D**, arrowheads). Overall, the frequency of ciliated cells with IFT88 aggregates was reduced by ~50% in infected Cby−/− ciliated cells (data not shown). These data confirm that the IFT88 accumulations are attributable to the loss of Cby and suggest that Cby is required for normal distribution of IFT88 along cilia.

Loss of Cby causes IFT88 mislocalization at the distal tip of primary cilia

IFT is a critical process for the generation and maintenance of both primary and multicilia.[1,3,5,46] We therefore examined IFT88 localization in a well-established model for primary ciliogenesis: serum-starved mouse embryonic fibroblasts (MEFs) that were derived from Cby+/+ and Cby−/− embryos between embryonic days 12.5 and 14.5.[59,60] Consistent with our findings in multiciliated cells, IFT88 accumulations were observed at the distal end of primary cilia with a significantly increased frequency in Cby−/− MEFs (42.3 ± 7 .9% of ciliated cells) compared to Cby+/+ MEFs (20.2 ± 3 .6% of ciliated cells) ($p < 0.05$; $n = 3$) (**Fig. 3A**, arrowheads, **and B**). These data indicate that Cby performs a similar function to regulate distribution of IFT-associated proteins in both primary and multicilia.

IFT88 accumulates in the bulge structure at the ciliary tips in Cby−/− airway ciliated cells

We suspected that the IFT88 accumulations in Cby−/− MTECs (**Fig. 2A**) might reflect IFT particle accumulation within the bulged, dilated ciliary tip structures as observed by SEM (**Fig. 1**). To resolve the exact location of these IFT88 aggregates, we utilized 3-dimensional structured illumination microscopy (3D-SIM) to image ALId21 Cby+/+ and Cby−/− MTECs co-stained with antibodies for IFT88 and acetylated α-tubulin (**Fig. 4**). 3D-SIM provides 2-fold increased resolution compared to conventional confocal microscopy in each of the x-, y-, and z-dimensions, which permits visualization beyond the diffraction limit. 3D-SIM imaging easily revealed that the large

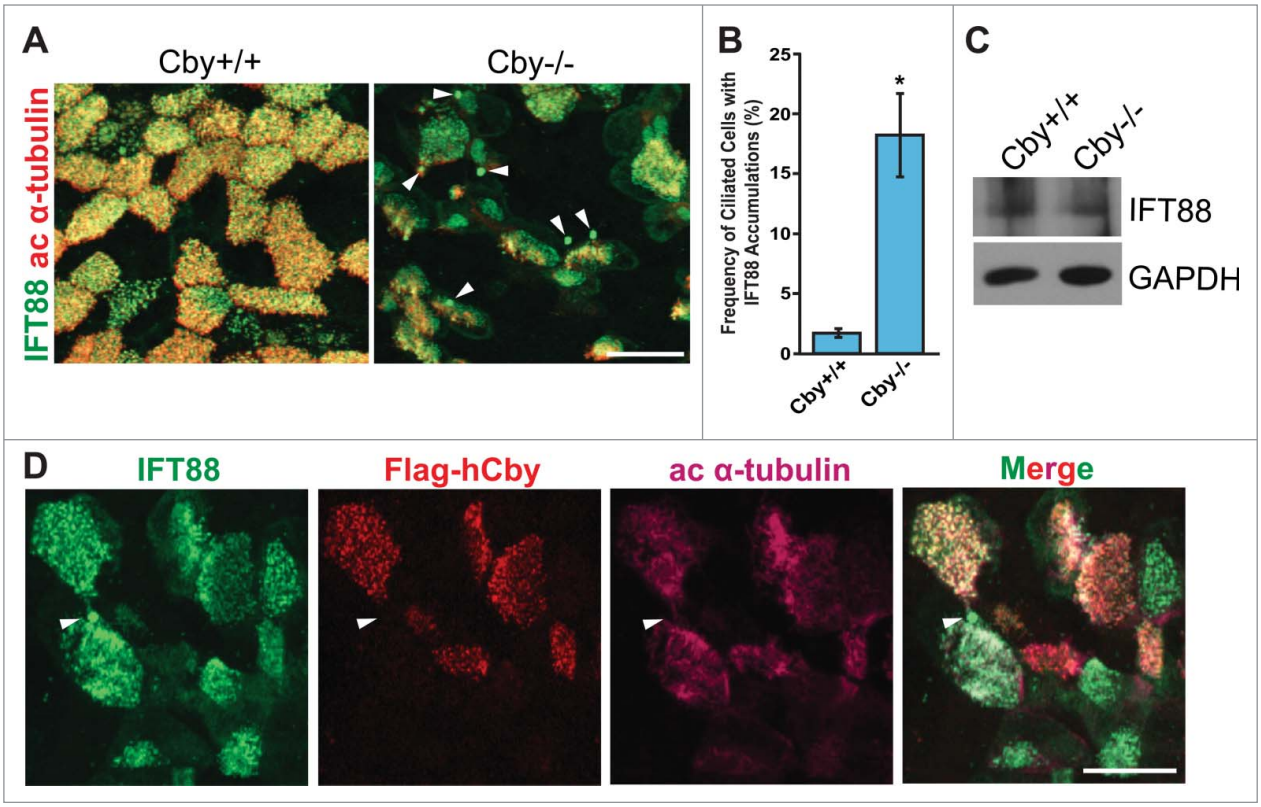

Figure 2. IFT88, a subunit of the IFT-B sub-complex, accumulates in Cby−/− tracheal ciliated cells. (**A**) Confocal images of Cby+/+ and Cby−/− MTECs at ALId21 colabeled for IFT88 (green) and the basal body/axonemal marker acetylated (ac) α-tubulin (red). Arrowheads indicate IFT88 accumulations in Cby−/− ciliated cells. Scale bar: 20 μm. (**B**) Quantification of frequency of ciliated cells with IFT88 accumulations in ALId21 Cby+/+ and Cby−/− MTECs. Greater than 250 ciliated cells were counted from each of 4 individual MTEC preparations. Data presented as means ± SEM. *, $p<0.05$. (**C**) Western blot analysis of IFT88 and GAPDH (loading control) from ALId21 Cby+/+ and Cby−/− MTEC lysates. No differences in IFT88 protein expression were observed. (**D**) Confocal images show ALId21 Cby−/− MTECs that were infected with lentiviruses that express Flag-tagged full-length human Cby (hCby) and were immunostained for IFT88 (green), Flag-hCby (red), and ac α-tubulin (magenta). Uninfected Cby−/− ciliated cells displayed IFT88 accumulations (arrowheads) while lentivirus-mediated expression of Flag-hCby rescued such accumulations. Scale bar: 20 μm.

IFT88 accumulations present in Cby−/− MTECs were enclosed within large, distended circular loops of acetylated α-tubulin-positive ciliary axonemes at the distal ends of cilia (**Fig. 4A and B**). Thus, it is likely that defects in IFT or inherent to IFT particles result in the accumulation of IFT particles at the ciliary tip and subsequent formation of paddle-like cilia.

In Cby−/− ciliated cells without large IFT88 masses, we observed a relatively normal IFT88 distribution pattern. However, moderate enrichment in IFT88 signal at the ciliary tip in Cby−/− MTECs was readily apparent upon 3D-SIM imaging (**Fig. 4C**). These moderate IFT88 accumulations were more frequent than the larger aggregates, suggesting that they may represent a precursor step to the formation of more pronounced paddle-shaped cilia.

Cby regulates ciliary localization of IFT-B sub-complex members in ciliated cells

The IFT complex consists of >20 subunits that are grouped into 2 distinct sub-complexes: the IFT-B and IFT-A sub-complexes.[24,28] As IFT88 is one of the IFT-B complex members, we speculated that other IFT-B and IFT-A sub-complex components might also be misregulated and accumulate within the bulges in Cby−/− ciliated cells. We therefore evaluated the ciliary localization of the IFT-B proteins IFT20 and IFT57 and the IFT-A protein IFT140 by IF staining (**Fig. 5**). IFT20, IFT57, and IFT140 all demonstrated normal localization patterns in ALId21 Cby+/+ MTECs as reported previously (data not shown).[61-63] In contrast, in ALId21 Cby−/− MTECs, the IFT-B proteins IFT20 and IFT57 showed robust accumulations (**Fig. 5**) that colocalized with the IFT88 aggregates that were found to correspond to the bulge structures by 3D-SIM imaging (**Fig. 4**). Interestingly, the IFT-A subunit IFT140 was not detectable as aggregates with IFT88 (**Fig. 5**, dotted line enclosures). Hence, solely the IFT-B, not IFT-A, proteins, and presumptively the sub-complex, accumulate at the dilated ciliary tips of Cby−/− ciliated cells. These observations suggest that IFT-B proteins are, most likely, not trafficked out of the ciliary compartment efficiently in Cby−/− ciliated cells despite apparently normal trafficking of IFT-A complex members. Thus, this raises the interesting possibility that Cby influences the proper rearrangement of IFT particles at the ciliary tip from anterograde to retrograde transport.

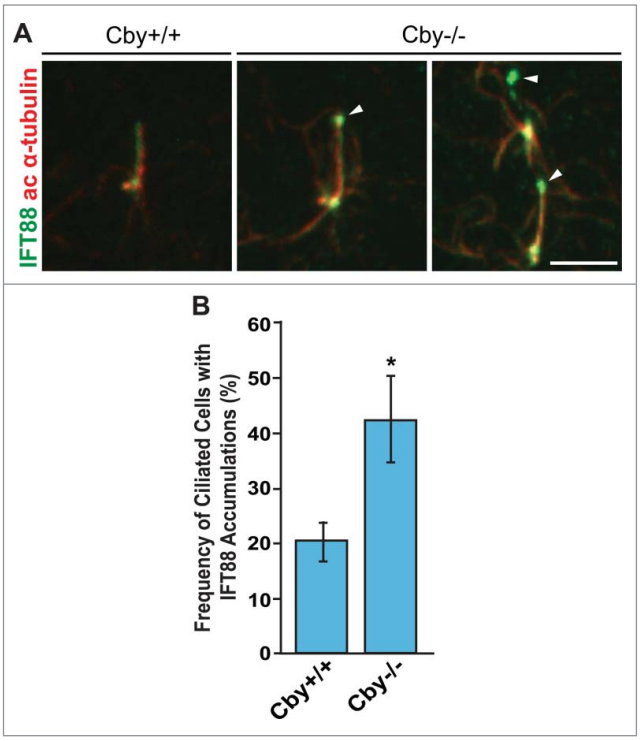

Figure 3. IFT88 aggregates at the distal tip of primary cilia are present in Cby−/− MEFs. (**A**) Confocal images of Cby+/+ and Cby−/− MEFs that were serum-starved for 48 hrs and stained for IFT88 (green) and ac α-tubulin (red). Accumulations of IFT88 (arrowheads) were found at the distal end of primary cilia in Cby−/− MEFs. Scale bar: 5 μm. (**B**) Quantification of frequency of ciliated cells with IFT88 accumulations in serum-starved Cby+/+ and Cby−/− MEFs. Greater than 198 cells with primary cilia were counted from each of 3 individual MEF preparations. Data presented as means ± SEM. *, $p < 0.05$.

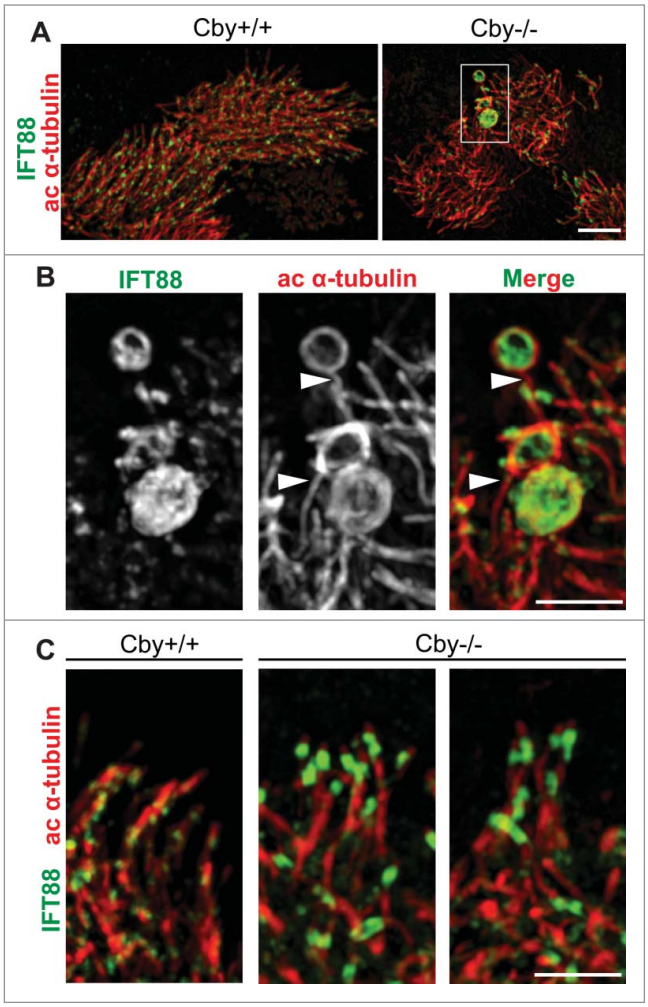

Figure 4. IFT88 accumulations are contained within the bulge structures at the dilated ciliary tips of Cby−/− tracheal ciliated cells. (**A**) Super-resolution 3D-SIM images of ALId21 Cby+/+ and Cby−/− MTECs colabeled for IFT88 (green) and ac α-tubulin (red). Scale bar: 5 μm. (**B**) Magnified images of the boxed area in (**A**) clearly demonstrate that IFT88 accumulations occurred within dilated ac α-tubulin-positive enclosures at the ciliary tip. Single channel images for IFT88 and ac α-tubulin staining are shown in grayscale. Ciliary axonemes, which harbor IFT88 accumulations, are indicated by arrowheads. Scale bar: 1 μm. (**C**) 3D-SIM images of cilia in Cby+/+ and Cby−/− MTECs at ALId21 colabeled for IFT88 (green) and ac α-tubulin (red). Moderate IFT88 accumulations at the ciliary tip were frequently found in Cby−/− ciliated cells. Note that IFT88 accumulations, large or small, were not seen in Cby+/+ cilia. Scale bar: 1 μm.

Similar to the airway bulge phenotype of Cby−/− mice, mouse mutants for the BBSome component BBS1, BBS2, BBS4, or BBS6 develop bulges filled with vesicular structures near the distal tips of cilia in airway epithelia.[57] Hence, we hypothesized that Cby might be required for the proper localization and function of the BBSome. To address this possibility, we performed IF staining for BBS4 and BBS5 in Cby−/− MTECs at ALId21 (**Fig. 6**). Surprisingly, neither BBS4 nor BBS5 demonstrated aberrant accumulation with IFT88 (**Fig. 6**, dotted line enclosures). Thus, Cby does not appear to regulate BBSome localization although we cannot rule out the possibility that other BBSome components might be mislocalized or that the BBSome might be dysfunctional in the absence of Cby.

Discussion

Here we present evidence that Cby is required for normal ciliary architecture and IFT localization in ciliated cells in airway epithelia and MTEC cultures. IFT is a bidirectional process that requires both IFT-B and IFT-A complexes and anterograde kinesin and retrograde dynein motor proteins.[22,28,46] Based on studies of mutant phenotypes and IFT particle dynamics, it has been proposed that a unique complement of both IFT-B and IFT-A transport and motor proteins mediates anterograde and retrograde IFT, respectively. This proposed model would necessitate that the anterograde IFT-B complex and kinesins carry retrograde IFT-A proteins and dyneins to the ciliary tip as cargo and that the retrograde IFT-A complex and dyneins transport the anterograde components back to the cytoplasm. Hence, massive rearrangement of the IFT particle and its associated proteins, including kinesins and dyneins, must take place at the ciliary tip

for proper ciliary extension and maintenance.[26,64] Thus, a failure to rearrange the IFT particle at the ciliary tip, as documented in IFT-A or BBSome mutants, leads to the formation of bulge structures.[47-49,51-53, 57] In the absence of Cby, the IFT-B component IFT88 accumulates within the bulged, dilated ciliary tips of both Cby−/− primary cilia and multicilia (**Figs. 2–4**). In agreement with this observation, the *D. melanogaster* IFT88 homolog is found to accumulate in the embryonic chordotonal cilia of the *Cby* mutant fly,[38] indicating that the function of Cby as an IFT regulator is evolutionarily conserved. Interestingly, solely other IFT-B sub-complex members amass with IFT88 in Cby−/− ciliated cells (**Figs. 5 and 6**), suggesting that anterograde IFT occurs normally in Cby−/− ciliated cells while IFT-B components are either not properly loaded as cargos onto the retrograde IFT complex or unable to effectively exit the ciliary compartment. Coupled with the normal localization pattern of IFT-A proteins and BBSome members, we speculate that Cby is important for a switch from anterograde to retrograde IFT at the ciliary tip.

The BBSome has been shown to be a critical effector of IFT and proposed to be involved in IFT particle turnaround at the ciliary tip.[26,27,29] Furthermore, several BBS mouse mutants display bulge phenotypes in airway ciliated cells strikingly similar to those in Cby−/− mice.[57] Hence, it is particularly surprising that both BBS4 and BBS5 demonstrated relatively normal distribution patterns in Cby−/− MTECs (**Fig. 6**). However, the possibility remains that other BBSome components may show altered distribution or that the BBSome may be dysfunctional in Cby−/− ciliated cells. Thus, a potential connection between the BBSome complex and Cby is clearly an intriguing area of potential future exploration.

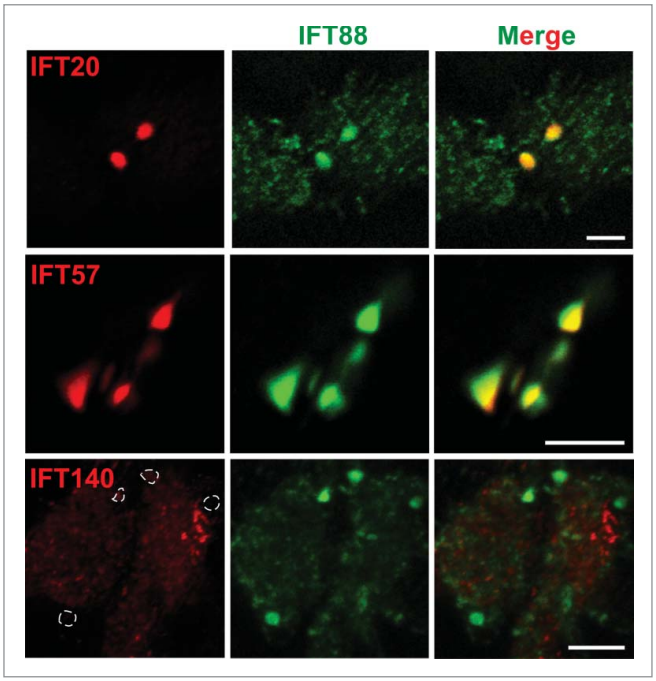

Figure 5. IFT-B sub-complex members exhibit localization patterns similar to IFT88 in Cby−/− tracheal ciliated cells. Shown are immunofluorescence confocal images of ALId21 Cby−/− MTECs stained for IFT88 (green) and either IFT-B sub-complex members IFT20 or IFT57 or IFT-A sub-complex member IFT140 (red), as indicated. IFT20 and IFT57 localized in patterns similar to IFT88 while IFT140 did not accumulate with IFT88. Dashed enclosures correspond to the areas positive for IFT88 accumulations. Scale bars: 5 μm.

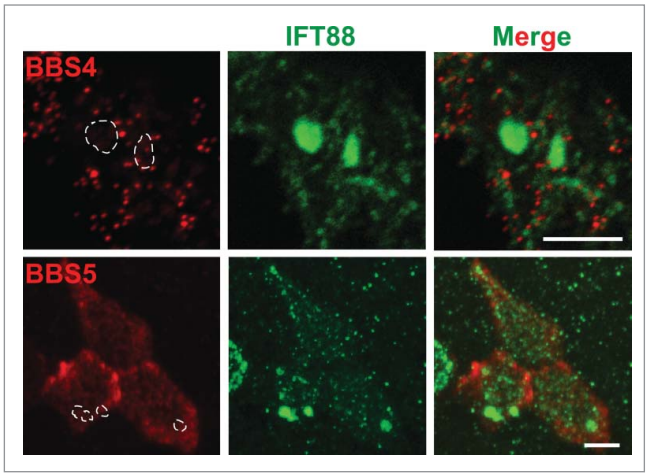

Figure 6. BBSome proteins are normally distributed and do not accumulate at the distal tips in Cby−/− ciliated cells. ALId21 Cby−/− MTECs were immunostained for IFT88 (green) and either BBS4 or BBS5 (red), as indicated. BBS4 and BBS5 did not accumulate in the areas positive for IFT88 aggregations (dashed enclosures). Scale bars: 5 μm.

How might Cby regulate IFT rearrangement at the ciliary tip? An attractive model is that Cby localizes to the ciliary compartment along cilia, travels with the IFT particle, and directly impacts IFT particle rearrangement at the ciliary tip. We attempted with the use of several methodologies to detect Cby in the ciliary compartment in MTECs by IF staining. Intense Cby signal was observed at the base of cilia, consistent with previous reports;[15,34-39] however, Cby was not clearly detectable in the ciliary compartment (data not shown). While it remains possible that the levels of Cby in the ciliary compartment are beyond the detection limit of our current methods, a more likely scenario is that Cby influences IFT particle assembly from its position at the ciliary base. Several lines of evidence support this proposal. Cby predominantly clusters around the transition fibers in mature ciliated cells,[15,34-39] which are known to be the sites critical for IFT particle assembly, docking, and entry into the ciliary compartment.[14,21] Interestingly, other transition fiber proteins, such as CEP164 and FBF1,[17,65-67] have also been shown to regulate IFT particle formation and ciliary entry, implying that particularly complex regulation of IFT processes may occur at the transition fibers. Thus, Cby may modulate recruitment of IFT components, assembly of IFT-motor complexes, and their efficient entry into the ciliary compartment at the ciliary base.

The trapping of IFT-B components at the ciliary tip is most likely a rate-limiting process, which accounts for the ~18% frequency with which we observe the more dramatic IFT88 accumulations (**Fig. 2B**). Furthermore, the accumulation of IFT88 in only a subset of cilia implies a considerable heterogeneity in IFT among individual cilia and, hence, an explanation why not all

cilia display overt morphological deficits at any given time. However, the more abundant presence of smaller IFT88 accumulations detectable with 3D-SIM imaging suggests an interesting model for bulge formation at the ciliary tip (**Fig. 4D**). We propose that, subsequent to axonemal extension in Cby−/− ciliated cells, IFT-B components accumulate at the ciliary tip due to defective retrograde trafficking of these IFT-B proteins. Thus, small accumulations of IFT-B proteins begin to form as a precursor state to the formation of larger accumulations of these IFT-B proteins, which cause bulge formation and paddle-like cilia. In support of this model, the frequency of large IFT88-positive bulges at the ciliary tips increased as Cby−/− MTEC cultures were maintained for longer periods of time (data not shown). However, it is also conceivable that these bulges form during the early phases of ciliogenesis before cilia fully elongate. Alternatively, small versus large IFT88 accumulations may reflect the severity of the deregulation of IFT particle assembly and rearrangement. Indeed, many predictions exist as the molecular underpinnings of how paddle-like cilia phenotypes develop are unclear.

Despite over 20 years elapsing since the discovery of IFT,[22,68] its complex regulation is still an area of much active research. Here, we propose that Cby is a regulator of IFT processes, including IFT particle assembly and rearrangement as its loss causes both mislocalization of IFT components and alterations in ciliary structure. However, the exact molecular basis by which Cby regulates IFT processes warrants further investigation to provide novel insight into where Cby fits into a larger IFT regulatory network. Additionally, further examination of the underlying mechanism by which loss of Cby results in the formation of paddle-like cilia may help us to understand both how cilia are formed and maintained as well as how IFT misregulation leads to defects in ciliary structure.

Materials and Methods

Mouse strains

The generation of Cby−/− mice has been previously described.[34] Cby+/+ or Cby−/− mice were obtained by intercrossing Cby+/− mice on a mixed C57BL/6J and 129/SvJ background. All mice were handled in accordance with NIH guidelines and protocols approved by the Institutional Animal Care and Use Committee of Stony Brook University.

Plasmids and reagents

The lentiviral expression construct for FLAG-hCby has been previously described.[15] Briefly, a cDNA encoding for FLAG-hCby was subcloned into a 2nd generation lentiviral transfer vector pEF1α-IRES-EGFP (gift from Dr. I. Lemischka, Mount Sinai Medical Center, New York, NY, USA). Lentiviruses were produced by transient transfection of HEK293T cells according to standard protocols. All chemicals were purchased from Sigma-Aldrich unless otherwise noted.

MTEC preparation

MTECs were prepared as previously described.[10,15,44] Briefly, tracheas from adult Cby+/+ or Cby−/− mice were collected and incubated overnight with 1.5 mg/mL pronase (Roche). Isolated tracheal epithelial cells were then seeded onto collagen-coated Transwell permeable membranes made of either polycarbonate or polyester (6.5 mm insert; Corning-Costar) and allowed to proliferate in MTEC Plus with retinoic acid (RA) media. For lentiviral infection, viral media were added with MTEC Plus media supplemented with RA at a 1:1 ratio in the apical chamber for the first 48 hrs after seeding. Fresh media and virus were provided after the first 24 hrs of infection. Upon achieving confluency, an air-liquid interface (ALI) was established with 2% NuSerum media with RA provided only in the basal chamber of the Transwell. The day that an ALI was created was considered ALI day 0 (ALId0). MTECs were maintained until ALId21 unless otherwise noted.

MEF preparation

Cby+/+ and Cby−/− MEFs were prepared from mouse embryos between embryonic days 12.5 and 14.5, as described previously.[69] MEFs were propagated in DMEM (Gibco) supplemented with 10% fetal bovine serum (Denville Scientific) and 100 U/mL penicillin-streptomycin (Gibco). To induce ciliogenesis, MEFs seeded on coverslips in a 24-well tissue culture plate were serum-starved for 48 hrs after reaching confluency.[60,69]

Western blotting

Western blotting was performed as previously described on Cby+/+ and Cby−/− ALId21 MTEC lysates.[70,71] The primary antibodies used were the following: rabbit anti-IFT88 (Proteintech) and mouse anti-GAPDH (Biodesign International).

Immunofluorescence staining and imaging

ALId21, unless otherwise noted, MTEC membranes or MEFs were washed with phosphate buffered saline (PBS) and fixed with methanol-acetone (used 1:1) on ice for 20 min. Membranes were then washed 3X in PBS and cut into quarters. Samples were blocked and permeabilized with 5% goat serum in antibody solution (PBS with 0.2% Triton X-100 and 5% bovine serum albumin) for 1 hr at room temperature. Primary antibodies were incubated in antibody solution at dilutions specified below overnight at 4°C. After PBS washes 3X, samples were blocked and permeabilized again for 1 hr at room temperature, followed by secondary antibody incubation for 1 hr at room temperature. All secondary antibodies were diluted with antibody solution and used at a dilution of 1:250. The primary antibodies used were: rabbit anti-IFT88 (1:250; Proteintech), mouse anti-IFT88 (1:250; Proteintech), rabbit anti-IFT20 (1:250; gift from G, Pazour, University of Massachusetts Medical School, Worcester, MA, USA), rabbit anti-IFT57 (1:500; Proteintech), rabbit anti-IFT140 (1:500; Proteintech), rabbit anti-BBS4 (1:500; gift from M. Nachury, Stanford University, Palo Alto, CA, USA), rabbit anti-BBS5 (1:200; Proteintech), mouse anti-Cby 27-11 (1:300; in-house),[72] mouse anti-acetylated α-tubulin (1:1000; Sigma-Aldrich). The secondary antibodies used were: DyLight 488-

conjugated goat anti-rabbit IgG (Vector Laboratories), DyLight 549-conjugated goat anti-mouse IgG (Jackson ImmunoResearch), DyLight 549-conjugated goat anti-rabbit IgG (Vector Laboratories), Alexa Fluor 647-conjugated goat anti-mouse IgG2b (Invitrogen), Alexa Fluor 488-conjugated goat anti-mouse IgG (Invitrogen). After PBS washes 3X, MTEC membranes were counterstained for 2 minutes with DAPI and rinsed with PBS 3X. Samples were then mounted with Fluoromount-G (SouthernBiotech), and images were obtained on a Zeiss LSM Meta 510 laser scanning confocal microscope with a 63X/1.4 NA objective or a Nikon N-SIM microscope with a 100X/1.4 NA objective. Confocal and SIM images were analyzed with using LSM Image Browser (Carl Zeiss) and Elements (Nikon), respectively, and further processed using Photoshop (Adobe).

Scanning electron microscopy

SEM was performed as previously described.[15,34,35] Briefly, adult lung tissues and ALId21 MTEC membranes were fixed with 2% paraformaldehyde and 2% glutaraldehyde in PBS and then dehydrated in a graded ethanol series to 100%. After dehydration, samples were processed through a graded series of ethanol-hexamethyldisilazane (HMDS; Electron Microscopy Sciences) to 100% HMDS. Preparations were then air-dried, mounted on scanning EM stubs, and sputter coated with gold prior to imaging with a scanning electron microscope (LEO1550; Carl Zeiss). Images were analyzed and processed with Photoshop as described above.

IFT88 Accumulation Frequency Analysis

Numbers of ciliated cells with and without IFT88 accumulations were counted on a Leica DMI6000B fluorescent microscope for both MTECs and MEFs. For each condition, numbers of ciliated cells with IFT88 aggregates were divided by total ciliated cells counted to obtain percentages. Separate MTEC and MEF preparations were considered as individual experiments. Percentages were averaged and analyzed with paired, 2-tailed t-tests for significance. A p-value <0.05 was considered significant.

Disclosure of Potential Conflicts of Interest

No potential conflicts of interest were disclosed.

Acknowledgments

We would like to thank the past and present members of the Takemaru and Li labs for insightful discussion and critical input in the development of this project and manuscript. We would also like to thank Steve Brody for helpful discussion regarding MTEC preparation, Greg Pazour for IFT20 antibody, and Max Nachury for BBS4 antibody.

Funding

This work was supported by NHLBI R01 HL107493 to K.-I. T. S.S.S. was also supported by the Stony Brook Medical Scientist Training Program Grant T32 GM008444-23. The purchase of the Nikon SIM was supported, in part, by NIH 1S10OD016405-01.

References

1. Bisgrove BW, Yost HJ. The roles of cilia in developmental disorders and disease. Development 2006; 133:4131-43; PMID:17021045; http://dx.doi.org/10.1242/dev.02595
2. Fisch C, Dupuis-Williams P. Ultrastructure of cilia and flagella - back to the future! Biol Cell 2011; 103:249-70; PMID:21728999; http://dx.doi.org/10.1042/BC20100139
3. Goetz SC, Anderson KV. The primary cilium: a signalling centre during vertebrate development. Nat Rev Genet 2010; 11:331-44; PMID:20395968; http://dx.doi.org/10.1038/nrg2774
4. Waters AM, Beales PL. Ciliopathies: an expanding disease spectrum. Pediatric Nephrol 2011; 26:1039-56; PMID:21210154; http://dx.doi.org/10.1007/s00467-010-1731-7
5. Brooks ER, Wallingford JB. Multiciliated Cells. Curr Biol 2014; 24:R973-R82; PMID:25291643; http://dx.doi.org/10.1016/j.cub.2014.08.047
6. Boon M, Jorissen M, Proesmans M, De Boeck K. Primary ciliary dyskinesia, an orphan disease. Eur J Pediatr 2013; 172:151-62; PMID:22777640; http://dx.doi.org/10.1007/s00431-012-1785-6
7. Tilley AE, Walters MS, Shaykhiev R, Crystal RG. Cilia Dysfunction in Lung Disease. Annu Rev Physiol 2015; 77:379-406; PMID:25386990.
8. Jord AA, Lemaitre AI, Delgehyr N, Faucourt M, Spassky N, Meunier A. Centriole amplification by mother and daughter centrioles differs in multiciliated cells. Nature 2014; 516(7529):104-7; PMID:25307055
9. Nigg EA, Stearns T. The centrosome cycle: Centriole biogenesis, duplication and inherent asymmetries. Nat Cell Biol 2011; 13:1154-60; PMID:21968988; http://dx.doi.org/10.1038/ncb2345
10. Vladar EK, Stearns T. Molecular characterization of centriole assembly in ciliated epithelial cells. J Cell Biol 2007; 178:31-42; PMID:17606865; http://dx.doi.org/10.1083/jcb.200703064
11. Klos Dehring DA, Vladar EK, Werner ME, Mitchell JW, Hwang P, Mitchell BJ. Deuterosome-mediated centriole biogenesis. Dev Cell 2013; 27:103-12; PMID:24075808; http://dx.doi.org/10.1016/j.devcel.2013.08.021
12. Sorokin SP. Reconstructions of centriole formation and ciliogenesis in mammalian lungs. J Cell Sci 1968; 3:207-30; PMID:5661997
13. Zhao H, Zhu L, Zhu Y, Cao J, Li S, Huang Q, Xu T, Huang X, Yan X, Zhu X. The Cep63 paralogue Deup1 enables massive de novo centriole biogenesis for vertebrate multiciliogenesis. Nat Cell Biol 2013; 15(12):1434-44
14. Reiter JF, Blacque OE, Leroux MR. The base of the cilium: roles for transition fibres and the transition zone in ciliary formation, maintenance and compartmentalization. EMBO Rep 2012; 13:608-18; PMID:22653444; http://dx.doi.org/10.1038/embor.2012.73
15. Burke MC, Li FQ, Cyge B, Arashiro T, Brechbuhl HM, Chen X, Siller SS, Weiss MA, O'Connell CB, Love D, et al. Chibby promotes ciliary vesicle formation and basal body docking during airway cell differentiation. J Cell Biol 2014; 207:123-37; PMID:25313408; http://dx.doi.org/10.1083/jcb.201406140
16. Joo K, Kim CG, Lee MS, Moon HY, Lee SH, Kim MJ, Kweon HS, Park WY, Kim CH, Gleeson JG, et al. CCDC41 is required for ciliary vesicle docking to the mother centriole. Proc Natl Acad Sci U S A 2013; 110(15):5987-92; PMID:23530209
17. Schmidt KN, Kuhns S, Neuner A, Hub B, Zentgraf H, Pereira G. Cep164 mediates vesicular docking to the mother centriole during early steps of ciliogenesis. J Cell Biol 2012; 199:1083-101; PMID:23253480; http://dx.doi.org/10.1083/jcb.201202126
18. Tanos BE, Yang HJ, Soni R, Wang WJ, Macaluso FP, Asara JM, Tsou MF. Centriole distal appendages promote membrane docking, leading to cilia initiation. Genes Dev 2013; 27:163-8; PMID:23348840; http://dx.doi.org/10.1101/gad.207043.112
19. Sorokin S. Centrioles and the formation of rudimentary cilia by fibroblasts and smooth muscle cells. J Cell Biol 1962; 15:363-77; PMID:13978319; http://dx.doi.org/10.1083/jcb.15.2.363
20. Lu Q, Insinna C, Ott C, Stauffer J, Pintado PA, Rahajeng J, Baxa U, Walia V, Cuenca A, Hwang YS, et al. Early steps in primary cilium assembly require EHD1/EHD3-dependent ciliary vesicle formation. Nat Cell Biol 2015; 17:228-240.
21. Deane JA, Cole DG, Seeley ES, Diener DR, Rosenbaum JL. Localization of intraflagellar transport protein IFT52 identifies basal body transitional fibers as the docking site for IFT particles. Curr Biol 2001; 11:1586-90; PMID:11676918; http://dx.doi.org/10.1016/S0960-9822(01)00484-5
22. Rosenbaum JL, Witman GB. Intraflagellar transport. Nat Rev Mol Cell Biol 2002; 3:813-25; PMID:12415299; http://dx.doi.org/10.1038/nrm952

23. Scholey JM. Intraflagellar transport. Annu Rev Cell Dev Biol 2003; 19:423-43; PMID:14570576; http://dx.doi.org/10.1146/annurev.cellbio.19.111401.091318
24. Bhogaraju S, Engel BD, Lorentzen E. Intraflagellar transport complex structure and cargo interactions. Cilia 2013; 2:10; PMID:23945166; http://dx.doi.org/10.1186/2046-2530-2-10
25. Taschner M, Bhogaraju S, Lorentzen E. Architecture and function of IFT complex proteins in ciliogenesis. Differentiation 2012; 83:S12-22; PMID:22118932; http://dx.doi.org/10.1016/j.diff.2011.11.001
26. Wei Q, Zhang Y, Li Y, Zhang Q, Ling K, Hu J. The BBSome controls IFT assembly and turnaround in cilia. Nat Cell Biol 2012; 14:950-7; PMID:22922713; http://dx.doi.org/10.1038/ncb2560
27. Zhang Q, Seo S, Bugge K, Stone EM, Sheffield VC. BBS proteins interact genetically with the IFT pathway to influence SHH-related phenotypes. Hum Mol Genet 2012; 21:1945-53; PMID:22228099; http://dx.doi.org/10.1093/hmg/dds004
28. Sung CH, Leroux MR. The roles of evolutionarily conserved functional modules in cilia-related trafficking. Nat Cell Biol 2013; 15:1387-97; PMID:24296415; http://dx.doi.org/10.1038/ncb2888
29. Williams CL, McIntyre JC, Norris SR, Jenkins PM, Zhang L, Pei Q, Verhey K, Martens JR. Direct evidence for BBSome-associated intraflagellar transport reveals distinct properties of native mammalian cilia. Nat Commun 2014; 5:5813; PMID:25504142; http://dx.doi.org/10.1038/ncomms6813
30. Nachury MV. Tandem affinity purification of the BBSome, a critical regulator of Rab8 in ciliogenesis. Methods Enzymol 2008; 439:501-13; PMID:18374185; http://dx.doi.org/10.1016/S0076-6879(07)00434-X
31. Nachury MV, Loktev AV, Zhang Q, Westlake CJ, Peranen J, Merdes A, Slusarski DC, Scheller RH, Bazan JF, Sheffield VC, et al. A core complex of BBS proteins cooperates with the GTPase Rab8 to promote ciliary membrane biogenesis. Cell 2007; 129:1201-13; PMID:17574030; http://dx.doi.org/10.1016/j.cell.2007.03.053
32. Zaghloul NA, Katsanis N. Mechanistic insights into Bardet-Biedl syndrome, a model ciliopathy. J Clin Invest 2009; 119:428-37; PMID:19252258; http://dx.doi.org/10.1172/JCI37041
33. Takemaru K, Yamaguchi S, Lee YS, Zhang Y, Carthew RW, Moon RT. Chibby, a nuclear β-catenin-associated antagonist of the Wnt/Wingless pathway. Nature 2003; 422:905-9; PMID:12712206; http://dx.doi.org/10.1038/nature01570
34. Voronina VA, Takemaru K, Treuting P, Love D, Grubb BR, Hajjar AM, Adams A, Li FQ, Moon RT. Inactivation of Chibby affects function of motile airway cilia. J Cell Biol 2009; 185:225-33; PMID:19364920; http://dx.doi.org/10.1083/jcb.200809144
35. Love D, Li FQ, Burke MC, Cyge B, Ohmitsu M, Cabello J, Larson JE, Brody SL, Cohen JC, Takemaru K. Altered lung morphogenesis, epithelial cell differentiation and mechanics in mice deficient in the Wnt/β-catenin antagonist Chibby. PloS one 2010; 5:e13600; PMID:21049041; http://dx.doi.org/10.1371/journal.pone.0013600
36. Lee YL, Sante J, Comerci CJ, Cyge B, Menezes LF, Li FQ, Germino GG, Moerner WE, Takemaru K, Stearns T. Cby1 promotes Ahi1 recruitment to a ring-shaped domain at the centriole-cilium interface and facilitates proper cilium formation and function. Mol Biol Cell 2014; 25:2919-33; PMID:25103236; http://dx.doi.org/10.1091/mbc.E14-02-0735
37. Steere N, Chae V, Burke M, Li FQ, Takemaru K, Kuriyama R. A Wnt/β-catenin pathway antagonist Chibby binds Cenexin at the distal end of mother centrioles and functions in primary cilia formation. PloS one 2012; 7:e41077; PMID:22911743; http://dx.doi.org/10.1371/journal.pone.0041077
38. Enjolras C, Thomas J, Chhin B, Cortier E, Duteyrat JL, Soulavie F, Kernan MJ, Laurencon A, Durand B. Drosophila chibby is required for basal body formation and ciliogenesis but not for Wg signaling. J Cell Biol 2012; 197:313-25; PMID:22508513; http://dx.doi.org/10.1083/jcb.201109148
39. Shi J, Zhao Y, Galati D, Winey M, Klymkowsky MW. Chibby functions in Xenopus ciliary assembly, embryonic development, and the regulation of gene expression. Dev Biol 2014; 395:287-98; PMID:25220153; http://dx.doi.org/10.1016/j.ydbio.2014.09.008
40. Feng S, Knodler A, Ren J, Zhang J, Zhang X, Hong Y, Huang S, Peranen J, Guo W. A Rab8 guanine nucleotide exchange factor-effector interaction network regulates primary ciliogenesis. J Biol Chem 2012; 287:15602-9; PMID:22433857; http://dx.doi.org/10.1074/jbc.M111.333245
41. Knodler A, Feng S, Zhang J, Zhang X, Das A, Peranen J, Guo W. Coordination of Rab8 and Rab11 in primary ciliogenesis. Proc Natl Acad Sci U S A 2010; 107:6346-51; PMID:20308558; http://dx.doi.org/10.1073/pnas.1002401107
42. Westlake CJ, Baye LM, Nachury MV, Wright KJ, Ervin KE, Phu L, Chalouni C, Beck JS, Kirkpatrick DS, Slusarski DC, et al. Primary cilia membrane assembly is initiated by Rab11 and transport protein particle II (TRAPPII) complex-dependent trafficking of Rabin8 to the centrosome. Proc Natl Acad Sci U S A 2011; 108:2759-64; PMID:21273506; http://dx.doi.org/10.1073/pnas.1018823108
43. Vladar EK, Brody SL. Analysis of ciliogenesis in primary culture mouse tracheal epithelial cells. Methods Enzymol 2013; 525:285-309; PMID:23522475; http://dx.doi.org/10.1016/B978-0-12-397944-5.00014-6
44. You Y, Richer EJ, Huang T, Brody SL. Growth and differentiation of mouse tracheal epithelial cells: selection of a proliferative population. Am J Physiol Lung Cell Mol Physiol 2002; 283:L1315-21; PMID:12388377; http://dx.doi.org/10.1152/ajplung.00169.2002
45. Hoh RA, Stowe TR, Turk E, Stearns T. Transcriptional program of ciliated epithelial cells reveals new cilium and centrosome components and links to human disease. PloS one 2012; 7:e52166; PMID:23300604; http://dx.doi.org/10.1371/journal.pone.0052166
46. Scholey JM. Intraflagellar transport motors in cilia: moving along the cell's antenna. J Cell Biol 2008; 180:23-9; PMID:18180368; http://dx.doi.org/10.1083/jcb.200709133
47. Huangfu D, Anderson KV. Cilia and Hedgehog responsiveness in the mouse. Proc Natl Acad Sci U S A 2005; 102:11325-30; PMID:16061793; http://dx.doi.org/10.1073/pnas.0505328102
48. Iomini C, Li L, Esparza JM, Dutcher SK. Retrograde intraflagellar transport mutants identify complex A proteins with multiple genetic interactions in Chlamydomonas reinhardtii. Genetics 2009; 183:885-96; PMID:19720863; http://dx.doi.org/10.1534/genetics.109.101915
49. Liem KF, Jr., Ashe A, He M, Satir P, Moran J, Beier D, Wicking C, Anderson KV. The IFT-A complex regulates Shh signaling through cilia structure and membrane protein trafficking. J Cell Biol 2012; 197:789-800; PMID:22689656; http://dx.doi.org/10.1083/jcb.201110049
50. Pazour GJ, Wilkerson CG, Witman GB. A dynein light chain is essential for the retrograde particle movement of intraflagellar transport (IFT). J Cell Biol 1998; 141:979-92; PMID:9585416; http://dx.doi.org/10.1083/jcb.141.4.979
51. Piperno G, Siuda E, Henderson S, Segil M, Vaananen H, Sassaroli M. Distinct mutants of retrograde intraflagellar transport (IFT) share similar morphological and molecular defects. J Cell Biol 1998; 143:1591-601; PMID:9852153; http://dx.doi.org/10.1083/jcb.143.6.1591
52. Qin J, Lin Y, Norman RX, Ko HW, Eggenschwiler JT. Intraflagellar transport protein 122 antagonizes Sonic Hedgehog signaling and controls ciliary localization of pathway components. Proc Natl Acad Sci U S A 2011; 108:1456-61; ; PMID:21209331; http://dx.doi.org/10.1073/pnas.1011410108
53. Tsao CC, Gorovsky MA. Tetrahymena IFT122A is not essential for cilia assembly but plays a role in returning IFT proteins from the ciliary tip to the cell body. J Cell Sci 2008; 121:428-36; PMID:18211962; http://dx.doi.org/10.1242/jcs.015826
54. Eggenschwiler JT, Anderson KV. Cilia and developmental signaling. Annu Rev Cell Dev Biol 2007; 23:345-73; PMID:17506691; http://dx.doi.org/10.1146/annurev.cellbio.23.090506.123249
55. Cole DG. The intraflagellar transport machinery of Chlamydomonas reinhardtii. Traffic 2003; 4:435-42; PMID:12795688; http://dx.doi.org/10.1034/j.1600-0854.2003.t01-1-00103.x
56. Porter ME, Bower R, Knott JA, Byrd P, Dentler W. Cytoplasmic dynein heavy chain 1b is required for flagellar assembly in Chlamydomonas. Mol Biol Cell 1999; 10:693-712; PMID:10069812; http://dx.doi.org/10.1091/mbc.10.3.693
57. Shah AS, Farmen SL, Moninger TO, Businga TR, Andrews MP, Bugge K, Searby CC, Nishimura D, Brogden KA, Kline JN, et al. Loss of Bardet-Biedl syndrome proteins alters the morphology and function of motile cilia in airway epithelia. Proc Natl Acad Sci U S A 2008; 105:3380-5; PMID:18299575; http://dx.doi.org/10.1073/pnas.0712327105
58. Yang TT, Hampilos PJ, Nathwani B, Miller CH, Sutaria ND, Liao JC. Superresolution STED microscopy reveals differential localization in primary cilia. Cytoskeleton 2013; 70:54-65; PMID:23125024; http://dx.doi.org/10.1002/cm.21090
59. Ocbina PJ, Anderson KV. Intraflagellar transport, cilia, and mammalian Hedgehog signaling: analysis in mouse embryonic fibroblasts. Dev Dyn 2008; 237:2030-8; PMID:18488998; http://dx.doi.org/10.1002/dvdy.21551
60. Archer FL, Wheatley DN. Cilia in cell-cultured fibroblasts. II. Incidence in mitotic and post-mitotic BHK 21-C13 fibroblasts. J Anat 1971; 109:277-92; PMID:5105129
61. Follit JA, Tuft RA, Fogarty KE, Pazour GJ. The intraflagellar transport protein IFT20 is associated with the Golgi complex and is required for cilia assembly. Mol Biol Cell 2006; 17:3781-92; PMID:16775004; http://dx.doi.org/10.1091/mbc.E06-02-0133
62. Pazour GJ, Baker SA, Deane JA, Cole DG, Dickert BL, Rosenbaum JL, Witman GB, Besharse JC. The intraflagellar transport protein, IFT88, is essential for vertebrate photoreceptor assembly and maintenance. J Cell Biol 2002; 157:103-13; PMID:11916979; http://dx.doi.org/10.1083/jcb.200107108
63. Sedmak T, Wolfrum U. Intraflagellar transport molecules in ciliary and nonciliary cells of the retina. J Cell Biol 2010; 189:171-86; PMID:20368623; http://dx.doi.org/10.1083/jcb.200911095
64. Qin H, Diener DR, Geimer S, Cole DG, Rosenbaum JL. Intraflagellar transport (IFT) cargo: IFT transports flagellar precursors to the tip and turnover products to the cell body. J Cell Biol 2004; 164:255-66; PMID:14718520; http://dx.doi.org/10.1083/jcb.200308132
65. Cajanek L, Nigg EA. Cep164 triggers ciliogenesis by recruiting Tau tubulin kinase 2 to the mother centriole. Proc Natl Acad Sci U S A 2014; 111(28):E2841-50; PMID:24982133
66. Oda T, Chiba S, Nagai T, Mizuno K. Binding to Cep164, but not EB1, is essential for centriolar localization of TTBK2 and its function in ciliogenesis. Genes Cells 2014; 19(12):927-40
67. Wei Q, Xu Q, Zhang Y, Li Y, Zhang Q, Hu Z, Harris PC, Torres VE, Ling K, Hu J. Transition fibre protein FBF1 is required for the ciliary entry of assembled

intraflagellar transport complexes. Nat Commun 2013; 4:2750; PMID:24231678
68. Kozminski KG, Johnson KA, Forscher P, Rosenbaum JL. A motility in the eukaryotic flagellum unrelated to flagellar beating. Proc Natl Acad Sci U S A 1993; 90:5519-23; PMID:8516294; http://dx.doi.org/10.1073/pnas.90.12.5519
69. Li FQ, Singh AM, Mofunanya A, Love D, Terada N, Moon RT, Takemaru K. Chibby promotes adipocyte differentiation through inhibition of β-catenin signaling. Mol Cell Biol 2007; 27:4347-54; PMID:17403895; http://dx.doi.org/10.1128/MCB.01640-06
70. Li FQ, Mofunanya A, Fischer V, Hall J, Takemaru K. Nuclear-cytoplasmic shuttling of Chibby controls β-catenin signaling. Mol Biol Cell 2010; 21:311-22; PMID:19940019; http://dx.doi.org/10.1091/mbc.E09-05-0437
71. Li FQ, Mofunanya A, Harris K, Takemaru K. Chibby cooperates with 14-3-3 to regulate β-catenin subcellular distribution and signaling activity. J Cell Biol 2008; 181:1141-54; PMID:18573912; http://dx.doi.org/10.1083/jcb.200709091
72. Cyge B, Fischer V, Takemaru K, Li FQ. Generation and characterization of monoclonal antibodies against human Chibby protein. Hybridoma (Larchmt) 2011; 30:163-8; PMID:21529289; http://dx.doi.org/10.1089/hyb.2010.0098